ChemPubSoc Europe

DOI: 10.1002/ejic.201901043

EurJIC European Journal of Inorganic Chemistry

Full Paper

Check for updates

Anticancer Organogold Complexes

SPECIAL ISSUE

Exploring the Reactivity and Biological Effects of Heteroleptic N-Heterocyclic Carbene Gold(I)-Alkynyl Complexes

Jens Oberkofler,[a,b,c] Brech Aikman,[b] Riccardo Bonsignore,[b] Alexander Pöthig,[a] James Platts,[b] Angela Casini,*[b,c] and Fritz E. Kühn*[a]

Abstract: With the aim to explore the effects of different organometallic ligands on the reactivity and biological properties of a series of twelve heteroleptic Au^{I} complexes, of general formula [Au(NHC)(alkynyl)] (NHC = benzimidazolylidene or 1,3-dihydroimidazolylidene) were synthesized and characterized by ^{1}H and ^{13}C NMR and elemental analysis, and in some cases also by X-ray diffraction. The compounds were all stable in H_2O/DMSO as established by NMR spectroscopy, while they could react with model thiols (EtSH) in the presence of water to undergo ligand-substitution reactions. ^{1}H NMR experiments showed that dissociation of the more labile alkynyl ligand was possible for all compounds, while in the case of the benzimidazolylidene series also dissociation of the NHC ligand could be observed. DFT calculations suggest that, depending on the steric hindrance exerted by both the NHC wingtip groups and the alkynyl substituents, the reaction can proceed either *via* a π-stabilized intermediate or with the alkynyl ligand remaining purely σ-coordinated to the Au^{I} center until completely dissociated. The most stable compounds in PBS buffer (pH 7.4), as assessed by UV-Visible spectrophotometry, were further investigated for their ability to stabilize G4 DNA by FRET DNA melting assay, showing only moderate activity. Moreover, two derivatives were tested *in vitro* for their anticancer activities in three different human cancer cell lines and showed cytotoxicity in the low micromolar range.

Introduction

As the World Health Organization states in its report, approximately 14 million new cases of cancer and 8 million cancer-related deaths were registered in the year 2012 alone, both numbers rising steadily and underpinning the urgency of development and improvement of new anticancer drugs.[1] The Pt^{II} complex cisplatin was approved by the FDA in 1978 and is still widely used in clinics against cancer, together with a number of analogues (e.g. carboplatin, oxaliplatin etc.).[2] Despite its success, the demand for new pharmaceuticals, including metal-based compounds, is on the rise since platinum compounds can cause severe side effects as well as build up resistances. In this context, the design of gold(I) and gold(III) compounds has attracted great attention as an alternative to the well-established platinum drugs.[3] While Au^{I} complexes generally feature a linear geometry, with the gold center coordinated by two ligands, Au^{III} compounds prefer a square-planar coordination and are isoelectronic (d^8) to the aforementioned Pt^{II} compounds.[4]

The stabilization of the oxidation states +I and +III in aqueous environment plays a key role in the design of biologically active gold compounds. In recent years N-heterocyclic carbenes (NHCs) have emerged as a particularly valuable family of ligands for the design of novel anticancer drugs.[5] The high stability of the metal–NHC bond leads to a lower risk of metabolization/speciation of the biologically active compound. Furthermore, the modification of the NHC ligand is significantly less challenging than in the case of phosphines or other types of ligands. Moreover, steric and electronic properties of the resulting metal NHC complexes are easily tunable and allow modulation of the compounds' solubility, lipophilicity, reactivity, stability and targeting properties.[6–9]

In general, gold compounds have lower affinity for nucleic acid binding with respect to Pt^{II} compounds, with a few exceptions. Instead, they primarily target proteins and enzymes, including the seleno-protein thioredoxin reductase (TrxR),[10] zinc finger proteins,[11] and the water and glycerol channels aquaporins,[12] among others.[13] In all cases, gold complexes have high affinity for binding to sulfur donors in proteins, including thiols of cysteine residues. Alternatively, our group has recently shown that some cationic bis-NHC Au^{I} compounds, endowed with high stability in aqueous environment, can target and sta-

[a] *Catalysis Research Center and Department of Chemistry, Technical University of Munich, Lichtenbergstraße 4, 85747 Garching, Germany*
E-mail: fritz.kuehn@ch.tum.de
https://www.department.ch.tum.de/molkat/prof-fritz-e-kuehn/
[b] *School of Chemistry, Cardiff University, Main Building, Park Place, Cardiff CF10 3AT, UK*
[c] *Department of Chemistry, Technical University of Munich, Lichtenbergstraße 4, 85747 Garching, Germany*
E-mail: angela.casini@tum.de
https://www.department.ch.tum.de/mbc/prof-angela-casini/

Supporting information and ORCID(s) from the author(s) for this article are available on the WWW under https://doi.org/10.1002/ejic.201901043.

bilize DNA secondary structures of pharmacological relevance, G-quadruplexes (G4s),[14] *via* a mechanism where no covalent, but rather π–π stacking and possibly electrostatic interactions take place between the compound and the nucleobases.[15]

To date, numerous Au^{I} NHC compounds with anticancer activities in the low micro- and nanomolar range have been reported.[6,7,9] Most compounds have been designed as neutral mono- {[Au(NHC)L], L = phosphine, thiol, etc.} or cationic bis-carbene {[Au(NHC)$_2$]$^+$} complexes, with modifications occurring at either of the three aforementioned positions (wingtip, backbone, ancillary ligand), with imidazole and benzimidazole as a core structure.[6] In this context, some of us reported on the anticancer properties of a heteroleptic NHC-Au-alkynyl complex featuring a *tert*-butylacetylene moiety as ancillary ligand.[16] The compound showed cytotoxicity in cancer cells *in vitro*, while being scarcely toxic in healthy rat kidney tissues *ex vivo*. More recently, we comparatively evaluated two novel families of Au^{I} bis-N-heterocyclic carbene and mixed NHC-alkynyl organometallics, featuring xanthine ligands, with respect to their stability in aqueous environment, G-quadruplex stabilizing effect and cytotoxicity.[17]

This work focuses on the synthesis, biological evaluation and systematic study of the reactivity of a new series of heteroleptic NHC-Au^{I}-alkynyl compounds by variation of the carbene core, the nitrogen wingtips, as well as the alkynyl ancillary ligand, to ensure different electronic and steric properties of the resulting Au^{I} compounds. Thus, the reactivity of the compounds with model thiols, as relevant intracellular nucleophiles, was investigated by ^{1}H NMR spectroscopy and DFT methods, while their stability in buffered solution was also preliminarily studied by UV-Visible spectroscopy. To elucidate the compounds' possible interaction with nucleic acids as relevant pharmacological targets, suitable Au^{I} complexes were additionally examined for their G4 DNA stabilization capabilities by Förster Resonance Energy Transfer (FRET) DNA melting assay. Finally, the antiproliferative properties of a few derivatives were tested in human cancer cells *in vitro*.

Results and Discussion

Synthesis and Characterization

In this work, a series of Au^{I} NHC complexes featuring alkynyl groups as ancillary ligands have been synthesized and characterized by different methods. Scheme 1 shows the general synthetic approach to NHC-Au^{I}-alkynyl compounds **1**–**12**. In the series, complexes **1**–**6** feature the benzimidazole (BzImi) scaffold, while complexes **7**–**12** the imidazolium (Imi) one. Compounds **1**,[18] **4**,[19] **7**,[20] **10**,[21] **11**[22] and **12**[22] have already been reported, and the synthetic procedures have been adapted here as necessary. In a first step, (benz)imidazolium

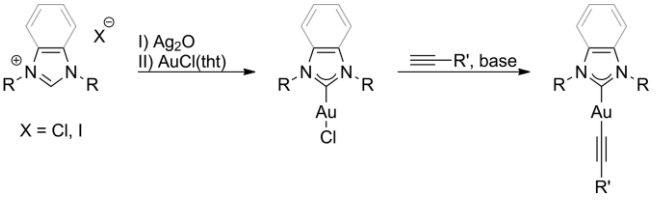

NHC: BzImi

1: R = Me R' = Ph
2: R = Me R' = Naph
3: R = Me R' = *t*-Bu
4: R = *i*-Pr R' = Ph
5: R = *i*-Pr R' = Naph
6: R = *i*-Pr R' = *t*-Bu

NHC: Imi

7: R = Mes R' = Ph
8: R = Mes R' = Naph
9: R = Mes R' = *t*-Bu
10 R = Dipp R' = Ph
11: R = Dipp R' = Naph
12: R = Dipp R' = *t*-Bu

Scheme 1. General synthetic approach to NHC-Au^{I}-alkynyl compounds **1**–**12**. BzImi= benzimidazolylidene; Imi = 1,3-dihydroimidazolylidene.

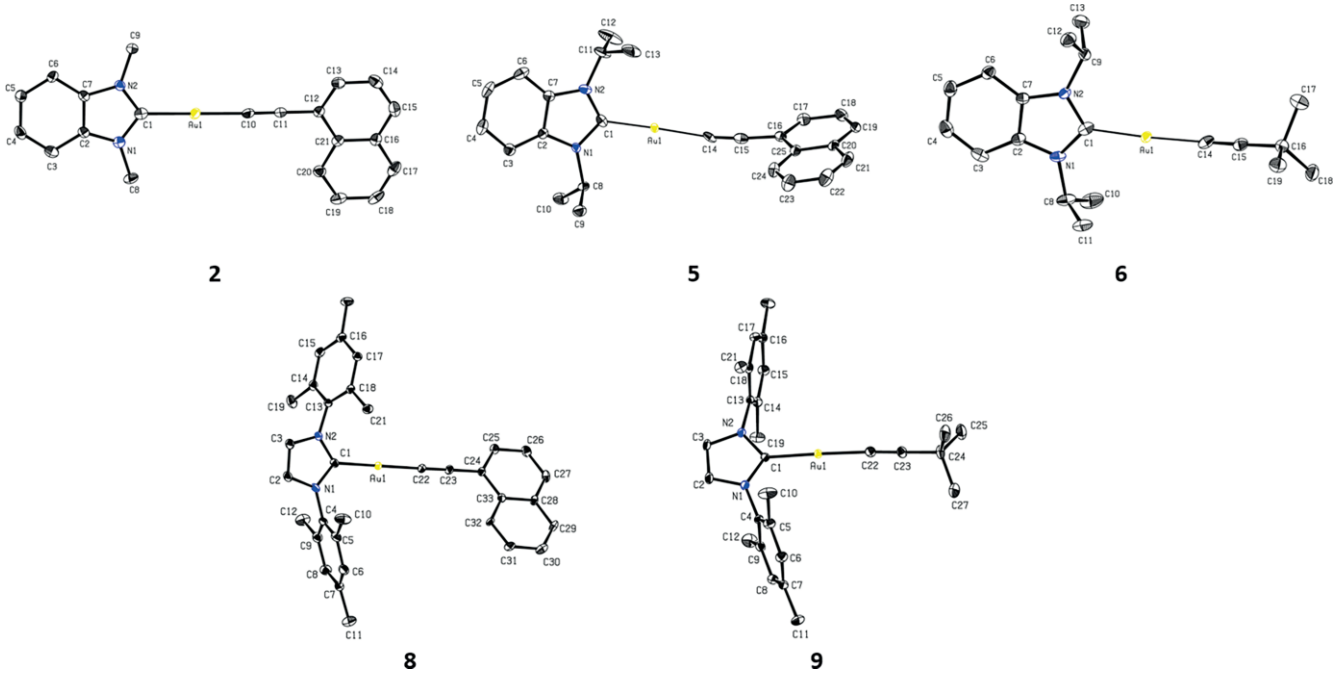

Figure 1. ORTEP style representation of **2**, **5**, **6**, **8** and **9** with ellipsoids shown at a 50 % probability level. Hydrogen atoms are omitted for clarity.

salts were converted to NHC-Au^{I}-Cl complexes by transmetalation *via* the corresponding silver analogue. In a second step, a base (NaOH or KO^{t}Bu) was used to deprotonate the alkyne which then undergoes a ligand exchange reaction with chloride to give the desired NHC-Au^{I}-alkynyl compounds **1**–**12** in moderate to good yields (27–90 %). The compounds were characterized by ^{1}H NMR and ^{13}C NMR spectroscopy, elemental analysis (EA) and single-crystal X-ray structure analysis (SC–XRD, compounds **2**, **5**, **6**, **8** and **9**).

All of the obtained X-ray structures display a classical linear, two-coordinated Au^{I} center as shown in Figure 1. The alkynyl substituents of **2**, **5** and **9** are tilted out of plane when compared to the NHC ligand with torsion angles of 3.89° (**2**), 71.41° (**5**) and 63.58° (**8**), respectively. A summary of selected bond lengths and angles can be found in Table 1, while full datasets are reported in Table S2 in the supplementary material. The C(1)–Au bond lengths are in the range of 1.985(4)-2.023(5) Å and the Au–C(sp) bond lengths between 1.987(5)-2.058(4) Å. The C(1)–Au–C(sp) angles are in the range of 172.81(15) - 179.4(2)°, deviating from an ideal 180° angle possibly due to crystal packing effects. The crystal lattice of compounds **5** and **6** show additional intermolecular Au···Au interactions in the range of 3.211 Å and 3.722 Å, respectively. Bond lengths, angles and intermolecular Au interactions are in accordance with previously reported structures.[19]

Table 1. Selected bond lengths and angles obtained by SC XRD.

Compound	C(1)–Au [Å]	Au–C(sp) [Å]	C(1)–Au–C(sp) [°]	Au···Au [Å]
2	2.023(5)	1.987(5)	179.4(2)	6.878
5	1.985(4)	2.058(4)	172.81(15)	3.211
6	1.997(3)	2.022(3)	173.75(14)	3.722
8	2.017(4)	1.987(3)	177.86(16)	7.234
9	2.009(2)	1.987(2)	177.12(18)	6.923

Reactivity with Thiols

As mentioned above, Au^{I} NHC complexes are likely to react with thiol groups of proteins, found in cysteine residues, which may be responsible for their cytotoxicity as well as for off-target effects (e.g. deactivation by intracellular thiols or binding to serum albumin). Therefore, the ligand exchange reaction of NHC-Au^{I}-alkynyl compounds in the presence of model thiols was investigated by NMR spectroscopy and density functional theory (DFT) methods.

Initially, all compounds were studied for their stability in the presence of water (see Fig. S25–S36). Each compound was dissolved in [D$_6$]DMSO/D$_2$O (80:20) and its stability monitored by ^{1}H NMR spectroscopy. The obtained results show that all compounds are stable with respect to hydrolysis over the course of two (**1**–**6**) or even nine days (**7**–**12**). Next, the reactivity of Au^{I} complexes with an excess of ethanethiol (EtSH), used as model

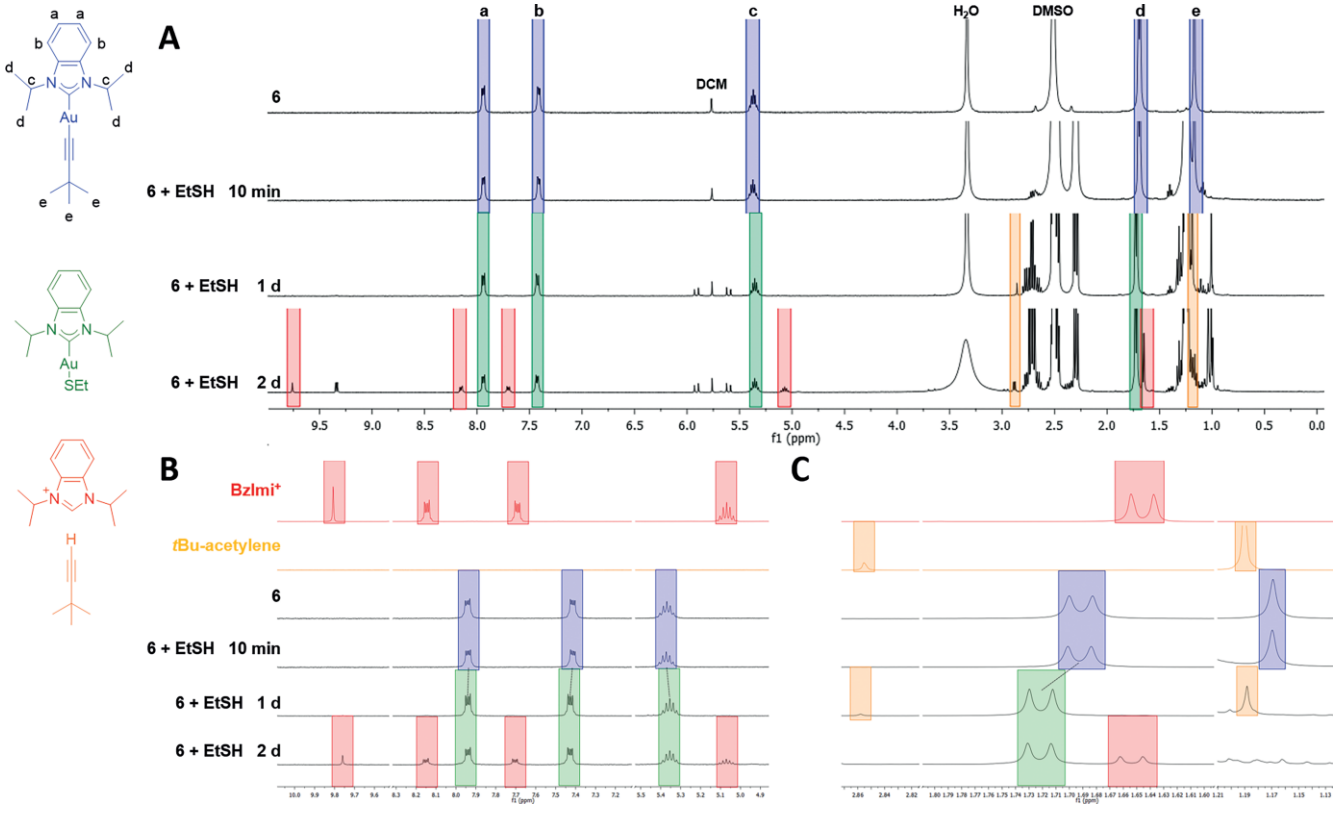

Figure 2. ^{1}H NMR spectra in [D$_6$]DMSO of compound **6** alone and in the presence of EtSH, recorded over time. **A** shows the whole spectra, **B** and **C** show selected cutouts between 4.90–10.0 ppm and 1.53–1.80 ppm, respectively. The spectrum of *t*Bu-acetylene and BzImi^{+} are shown for comparison (panels **B** and **C**). The color code in the NMR spectra matches the signals of the products depicted on the left.

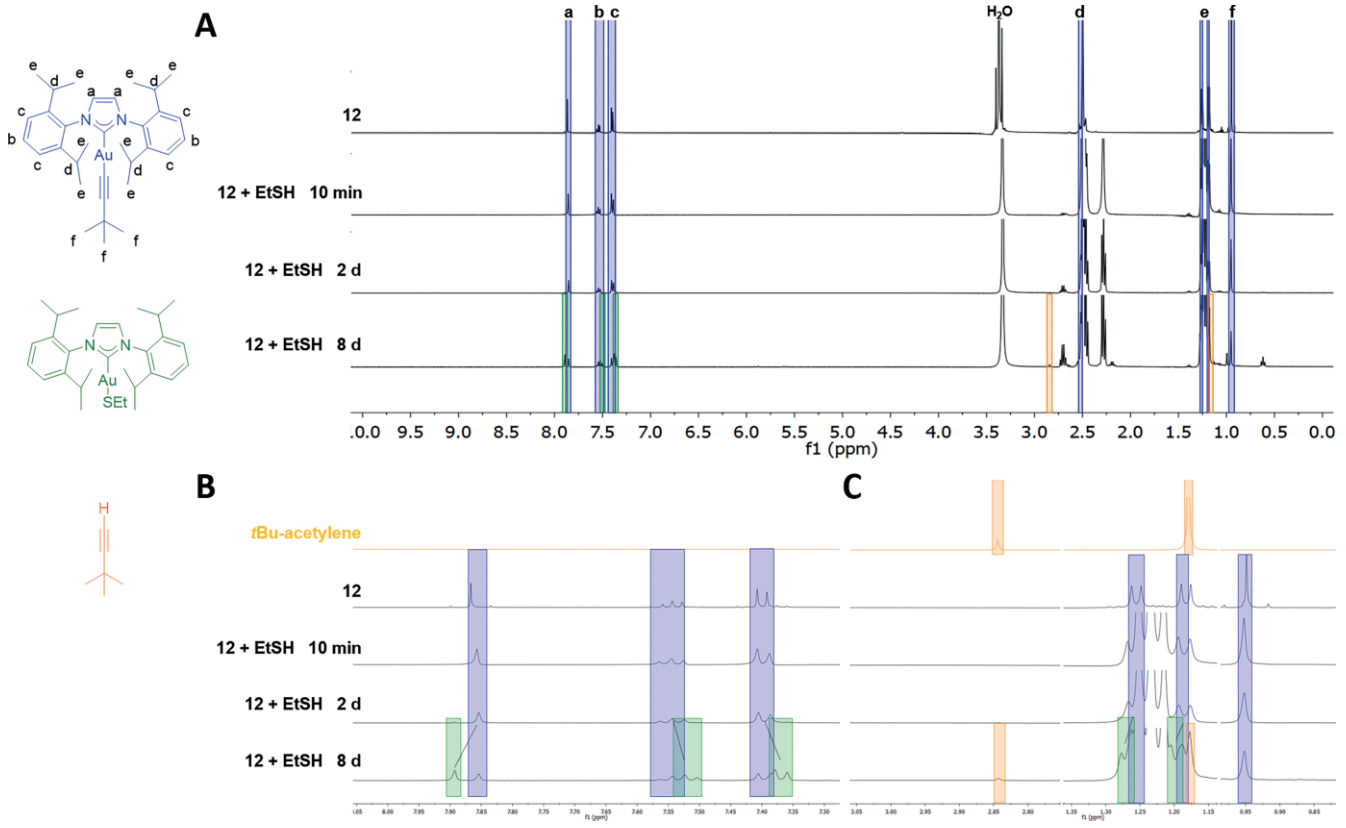

Figure 3. ^{1}H NMR spectra in [D_6]DMSO of compound **12** alone and in the presence of EtSH, recorded over time. Panel **A** shows the whole spectra, **B** and **C** show selected cutouts between 7.30–8.00 ppm and 0.85–3.00 ppm, respectively. The spectrum of *t*Bu-acetylene is shown for comparison (panels **B** and **C**). The color code in the NMR spectra matches the signals of the products depicted on the left.

thiol, was monitored by ^{1}H NMR spectroscopy in [D_6]DMSO (Figure 2 and Figure 3 and Fig. S37–S45). Concerning the benzimidazolylidene series, Figure 2 shows representative spectra for compound **6** recorded before and after addition of EtSH over two days. After 24 h, the aromatic signals experience a small downfield shift (from 7.93 and 7.42 ppm to 7.94 and 7.43 ppm, respectively), while the CH-signal of the isopropyl group undergo an upfield shift (from 5.38 to 5.36 ppm) and the CH_3-signal of the isopropyl group a downfield shift (from 1.69 to 1.72 ppm). Additional signals are observed in the spectrum of **6** recorded after 2 days, which were attributed to possible gold catalyzed alkyne activation.[23] Compounds **2** and **3** (Me-BzImi) feature similar spectral changes over time (Fig. S38 and S39), as well compounds **4** and **5** (Fig. S40 and S41), which all share the same benzimidazolylidene NHC ligand (*i*Pr-BzImi) as **6**. These variations are attributed to the formation of the NHC-Au^I-SEt adduct (Scheme 2), and are in line with previous studies on the reactivity of Au NHCs with model thiols.[16,24] Instead, complex **1** behaves differently and undergoes the loss of the BzImi ligand already after 5 h (Figure S37).

Furthermore, in the case of **6**, the signal of the *tert*-butylacetylene group (1.16 ppm) disappears within 24 h (Figure 2). In concomitance, signals of free alkyne appear (at 1.18 and 2.85 ppm), confirming the displacement of the alkynyl ligand, leading to the formation of NHC-Au–SEt and free alkyne. After two days, a second set of signals can be observed (at 9.75, 8.14, 7.69, 5.06 and 1.64 ppm) matching the signals of the free

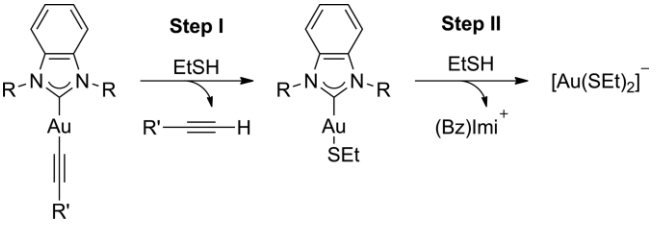

Scheme 2. Reactivity of BzImi-Au^I-alkynyl compounds **2**–**6** in the presence of the soft Lewis base EtSH. For the Imi-Au^I-alkynyl complexes (**7–12**), the reaction stops after Step I.

benzimidazolium salt, indicating the displacement of the NHC ligand possibly by a second equivalent of EtSH. This is also observed in the spectra of complexes **2**–**5** (Fig. S38–S41).

In all cases, we exclude formation of cationic bis-carbene products which would give rise to charcateristic NMR signals of the benzimidazole aromatic backbone in the range of 7.0–8.0 ppm. As representative examples, we report the spectra of the [Au(Me-BzImi)$_2$]$^+$ and [Au(*i*Pr-BzImi)$_2$]$^+$ derivatives in Figures S37 and S40.

Concerning the 1,3-dihydroimidazolylidene series (**7–12**), Figure 3 shows representative spectra for compound **12** recorded before and after addition of EtSH over a period of eight days. Only after this time, a second set of signals can be observed (7.89 ppm, 7.53 ppm, 7.36 ppm, 1.26 ppm, 1.19 ppm) matching the signals in the ^{1}H NMR spectra of compounds **10**

and **11** (Fig. S44 and S45), which all share the same (Dipp)Imi-NHC motif. Compounds **7** and **9** feature similar spectral changes after 2 and 8 days (Fig. S42 and S43). In concomitance, signals of free *tert*-butylacetylene can be observed (2.84 ppm, 1.18 ppm), indicating the displacement of the alkynyl ligand upon formation of a NHC-Au^{I}-SEt complex. Previous studies by our group showed that **12** undergoes a similar reaction with DL-homocysteine, where the alkynyl ligand is displaced by the thiol nucleophile. In the latter case, however, the reaction proceeds faster and is completed within 24 h.[16]

In general, all the investigated Au^{I} compounds, except for compound **1**, show a similar reaction pattern, where the thiol displaces the more labile alkynyl ligand (Step I, Scheme 2). Thus, compounds **2**–**6** show full conversion to the corresponding NHC-Au^{I}-SEt compound after one (**2**, **3**, **5**, **6**) or two days (**4**). For compounds **2**–**6**, a second reaction step (Step II, Scheme 2) could also be observed involving the displacement of the more stable NHC ligand. Compounds sharing the Imi type NHC ligand show different behaviors concerning their stability. While **7** and **10** (both sharing the phenylacetylene ligand) show full conversion to the corresponding NHC-Au^{I}-SEt after two days (**7**) and one day (**10**), respectively, compound **11** already reacts remarkably slower, with the reaction being completed only after four days. Interestingly, especially compounds **9** and **12** show high stability against EtSH. For compound **9** the reaction to the corresponding NHC-Au^{I}-SEt takes eight days, while the reaction of compound **12** is not completed even after this time. The reactivity of compound **8** with EtSH could not be determined by ^{1}H NMR spectroscopy due to its scarce solubility in [D$_6$]DMSO. In general, the bulkier the wingtip groups of the compound and the alkynyl ligand, the slower its reaction with EtSH.

It has to be noted that both the EtSH and the [D$_6$]DMSO used in the experiments contained traces of water. Therefore, in order to achieve a better understanding of the role of water molecules during the mechanism, reactivity studies with compound **6** were carried out with dry EtSH in dry [D$_6$]DMSO. In this case, the reaction proceeds only very slowly (see Fig. S46). While the displacement of the alkynyl ligand is already completed after one day in the presence of water, almost no reaction takes place in the absence of water after two days and only a 30 % conversion can be observed after eight days.

To explore the reactivity of the Au^{I} complexes with thiols and the underlying mechanism at a molecular level, DFT calculations were conducted on compounds **3** and **12**, as representative members of the two series, reacting with methanethiol (MeSH). One molecule of water was included in the mechanism as shown in Figure 4. In an initial step, compound **3** undergoes the concomitant activation of the alkynyl bond by the Au^{I} ion and the nucleophilic attack to the Au^{I} center by the thiol, while the water molecule acts as a proton shuttle to transfer a proton from the thiol group to the alkynyl ligand to give intermediate **I** (Figure 4A).

This process goes *via* a trigonal planar transition state **TS1** with an activation energy of 108.2 kJ/mol. Few examples of neutral, trigonal-planar coordinated Au^{I} compounds, where an alkynyl ligand is π coordinated to the gold center, have been reported before.[25] The activation energies and geometries of

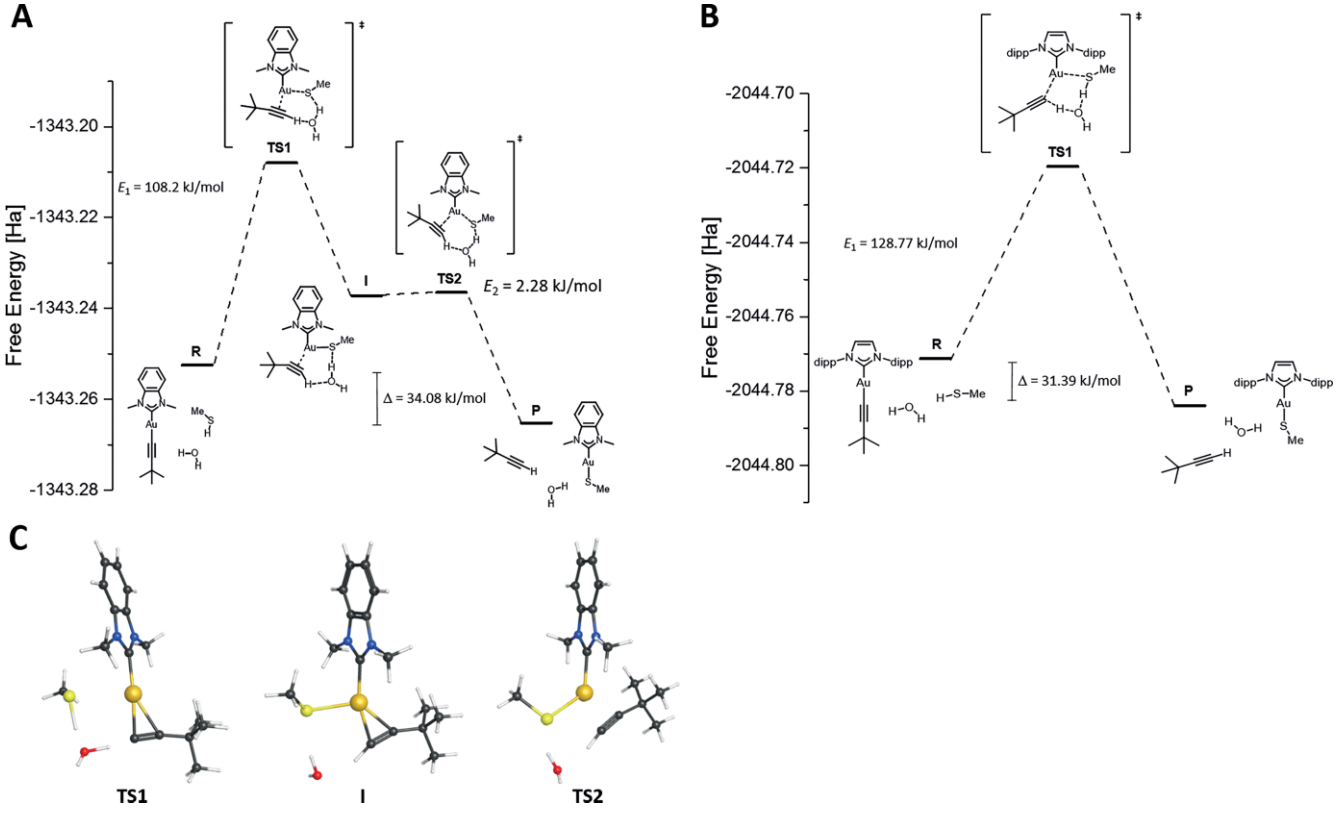

Figure 4. Mechanism of the reaction of compounds **3** (**A**) and **12** (**B**) with MeSH. Molecular representation of **TS1**, **I** and **TS2** (**C**).

the transition states are in accordance to previously reported DFT studies on similar NHC-Au^{I}-Cl complexes with protein targets.[26] In a second step, compound **3** undergoes complete dissociation of the alkynyl ligand and formation of the NHC-Au^{I}-SMe complex *via* another trigonal planar transition state **TS2**, with a very small activation barrier of 2.28 kJ/mol.

In contrast, compound **12** proceeds towards the formation of NHC-Au^{I}-SEt without an intermediate *via* a trigonal planar transition state (**TS1**, Figure 4B), while showing a higher activation barrier of 128.77 kJ/mol. While the Au–C(sp) and the Au–S bond lengths of the two transition states are comparable (2.208 Å and 3.175 Å for compound **3**, and 2.156 Å and 2.991 Å for compound **12**), the Au–C(*t*Bu) bond length and the Au–C(sp)–C(*t*Bu) bond angle differ greatly (2.406 Å and 83.236° for compound **3**, and 3.127 Å and 132.470° for compound **12**). The difference in activation energy can, therefore, be explained by the difference in stabilization of the transition states. While the transition state of compound **3** is not sterically hindered and can undergo a favorable π-stabilization, the alkynyl ligand of compound **12** remains purely σ coordinated to the Au^{I} center, due to the steric hindrance due to the respective NHC and alkynyl ligands (Figure 5). The higher energy barrier of compound **12** for the dissociation of the alkynyl ligand is in agreement with the experimental NMR data.

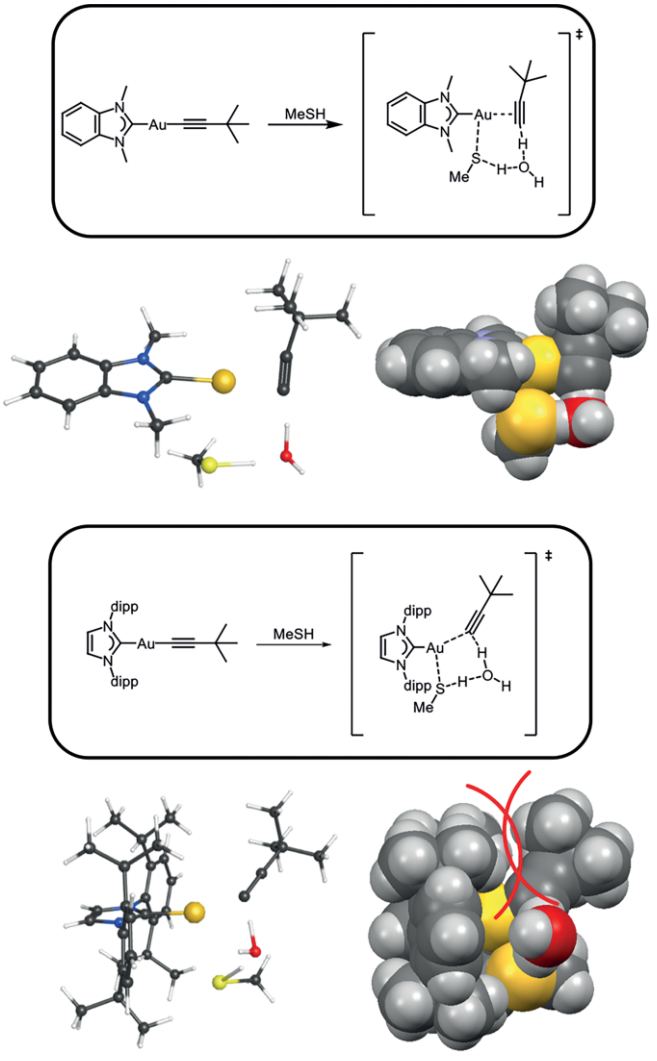

Figure 5. Transition states of compounds **3** and **12** and their *spacefill* style representations.

Stability in Buffered Solution

Compounds **1**–**12** were tested for their stability in a DMSO/PBS (pH 7.4, DMSO <2 %) solution by UV-Vis spectroscopy over 4 h at room temperature. The resulting absorption spectra feature bands in the range of 250–350 nm due to the organic ligands which undergo hypochromic shifts over time (Fig. S47–S48). A general trend of stability can be observed regarding the possible hydrolysis of the alkynyl ligands in the first hours. Specifically, the rate of compounds' degradation/hydrolysis seems to be more influenced by the type of alkynyl group than by the NHC scaffold (BzImi vs. Imi). The phenyl-substituted Au^{I} compounds (**1**, **4**, **7**, **10**) are the least stable in buffer, undergoing extensive decomposition within the first hour, possibly followed by precipitation, as shown by the progressive disappearance of the main absorption bands. The naphthyl-substituted Au^{I} compounds (**2**, **5**, **8**) are slightly more stable but still prone to hydrolysis/precipitation within 4 h. Finally, the *tert*-butyl-substituted Au^{I} compounds (**3**, **6**, **9**) are the most stable and only the imidazole-based compound **9** undergoes extensive reduction of the absorption bands after 4 h incubation (Fig. S48). An exception to this general trend is constituted by the *tert*-butyl-substituted Au^{I} complex (**12**), showing marked hypochromic spectral changes within 4 h.

FRET DNA Melting Assay

Afterwards, the BzImi-based compounds **2**–**6** were selected for FRET DNA melting analysis due to their extended π system, which make them possible candidates for the stabilization of G4 DNA. In details, hTelo and *C-KIT1* were chosen as models of telomeric and promoter G4 DNA, respectively. As shown in Figure 6 and Table S1, only compound **3** shows a significant G4 stabilizing effect, stabilizing hTelo by 3.51 (±0.08) °C and *C-KIT1* by 7.00 (±0.05) °C. While the compound is less effective than the benchmark bis-NHC Au^{I} complex [Au(9-methylcaffein-8-ylidene)$_2$]$^+$ (ΔT_m = 13.26±0.60 and 17.44±0.85 °C for hTelo and *C-KIT1*, respectively) it is certainly more effective than the previously reported mono-caffeine Au^{I} alkynyl analogues which showed no G4 stabilization.[17]

Antiproliferative Activity

Finally, two of the new compounds (**3** and **9**) were tested for their antiproliferative effects against human cancer cells *in vitro*, using the classical MTT assay (see Experimental for details). The preliminary data are compiled in Table 2 in comparison to the values previously reported for compound **12**.[16] The results show that the compounds are moderately active, with EC_{50} values in the low μM range, although having a certain selectivity with respect to the various cancer cell lines. For example, com-

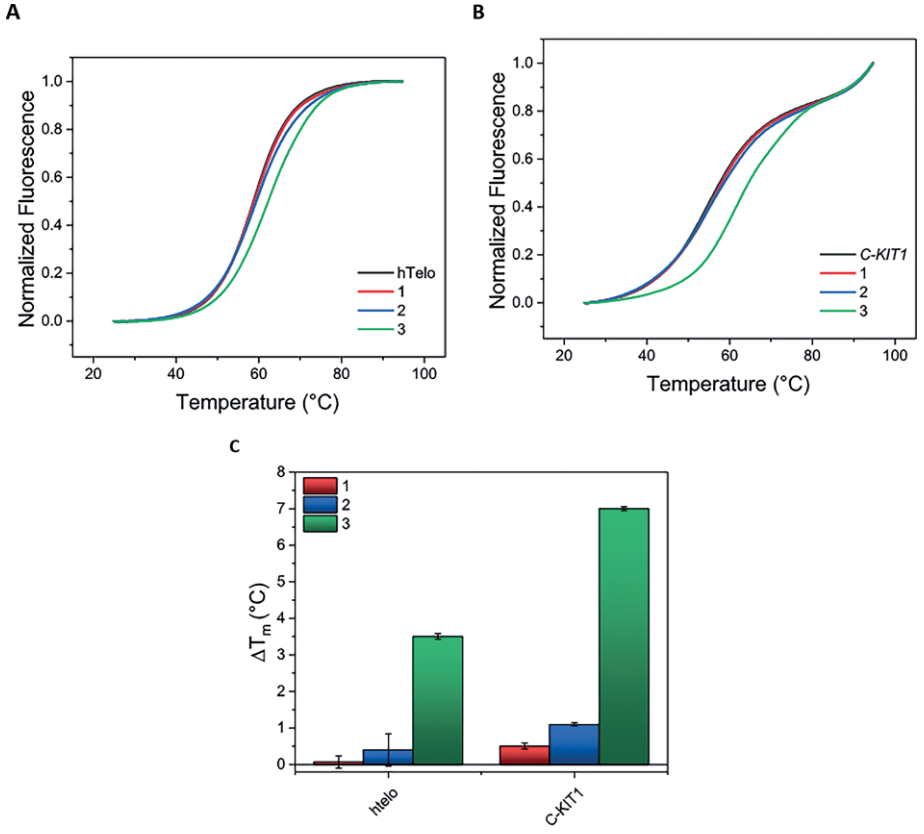

Figure 6. Representative FRET DNA melting profiles of 0.2 μM hTelo (**A**) and *C-KIT1* (**B**) G4-DNA solutions in 60 mM potassium cacodylate (pH = 7.4) in presence of 5 equiv. of selected Au^{I} NHC compounds **1**–**3**; (**C**) ΔT_m [°C] of hTelo and *C-KIT1* G4-DNA solutions in 60 mM potassium cacodylate (pH = 7.4) in presence of 5 equiv. of **1**–**3**. Data are shown as mean ± SEM of three independent experiments.

pound **9** is particularly active against the melanoma A375 cell line (EC_{50} = 3.4 ± 0.5 μM), comparable to cisplatin.

Table 2. EC_{50} values of heteroleptic NHC-Au^{I}-alkynyl complexes in human cancer cell lines, in comparison to cisplatin, after 72 h incubation.[a]

Compound	SKOV-3 (ovarian)	MCF-7 (breast)	A375 (skin)
3	13 ± 3	7.6 ± 0.8	12 ± 4
9	12 ± 2	7.1 ± 0.9	3.4 ± 0.5
12	n.d.	6 ± 2[b]	10 ± 1[b]
cisplatin	13.2 ± 2.4	12 ± 2	3.7 ± 0.9

[a] The reported EC_{50} values were calculated using a nonlinear fitting of log[concentration] vs. response and are presented as a mean (± SD) of at least three independent experiments; n.d.: not determined. [b] Data taken from ref.[16]

Conclusions

In this work, a small library of NHC-Au^{I}-alkynyl complexes with different substituents on the NHC scaffold as well as on the alkynyl ligand have been synthesized and fully characterized by different methods. Stability studies show that all compounds are stable in a mixture DMSO/H_2O as evidenced by ^{1}H NMR spectroscopy, but react in the presence of EtSH, leading in most cases, with the exception of compound **1**, to the nucleophilic substitution of the alkynyl ligand by the thiol group (Step I). Of note, the BzImi-Au^{I}-alkynyl complexes, upon EtSH binding, can also undergo the detachment of the NHC ligand over time (Step II). It is also worth noting that all the aforementioned ligand-substitution reactions are relatively slow in the applied experimental conditions (i.e. days), and that the presence of H_2O is necessary to initiate the nucleophilic substitution by EtSH.

DFT calculations led to a consistent mechanism for the title reaction (Step I) and the optimized geometries reveal that the transition state of the Au^{I} complexes reacting with EtSH exhibits trigonal planar configuration, in accordance with previous studies on bis-NHC Au^{I} complexes and cysteine-thiols.[27] In the case of the BzImi series, a trigonal reaction intermediate **I** is also identified, which can then easily progress towards the final Bzi-Au^{I}-SEt product.

Overall, NMR studies and DFT calculations suggest that the stability of the compounds with respect to EtSH is primarily influenced by: i) the type of NHC scaffold (BzImi vs. Imi), ii) the type of NHC wingtip groups and iii) the substitution at the alkynyl ligand. Specifically, the BzImi-based complexes (**1–6**) show full conversion into BzImi-Au^{I}-SEt adducts after one or two days independently on the type of NHC or alkynyl derivatization. Instead, the reactivity of the Imi-based compounds with EtSH varies depending on the steric hindrance between the NHC wingtip groups and the alkynyl substituents, during the transition state of the reaction, with **9** [(Mes)-Au^{I}-(*tert*-butylacetylene)] and **12** [(Dipp)-Au^{I}-(*tert*-butylacetylene)] being the most stable for at least 8 days.

All compounds were further tested for their stability in PBS (pH 7.4) to mimic the biological conditions. In these conditions, the compounds' possible decomposition/precipitation appears to be favored with respect to the aforementioned NMR studies, occurring in few hours. Moreover, the stability of the compounds in buffer seems to be more influenced by the type of alkynyl ligand rather than by the NHC scaffold. A general stability trend (with respect to the alkynyl substitution) of phenyl < naphthyl < *t*Bu can be observed, with *t*Bu being the most stable.

In conclusion, the mechanism of reactivity of heteroleptic NHC-Au^{I}-alkynyl compounds is extremely complex and further studies are necessary to be able to draw complete structure-activity relationships and to understand the role of water molecules and buffer components in the different possible pathways.

Finally, concerning the cytotoxic activity, preliminary results show that compounds **3** and **9** are only moderately active *in vitro* against all the tested cancer cell lines, comparable to cisplatin. The moderate cytotoxic effect is in line with the compounds' scarce reactivity with DNA G-quadruplexes and model thiols. Together with previously reported compound **12**, these results are among the few examples of heteroleptic NHC-Au^{I}-alkynyl compounds showing antiproliferative effects. In the future, other families of Au^{I} NHC carbenes should be studied for their biological effects, including based on triazole and tetrazole scaffolds, which are still rare in the literature,[28] but endowed with different reactivity profiles.

Experimental Section

General Remarks: Reactions were carried out without taking special precautions to exclude air and water. All chemicals were used as received. Solvents were distilled prior to use. NHC-Au^{I}-Cl complexes were synthesized by previously reported routes: Chloro(1,3-diisopropylbenzimidazolin-2-ylidene)gold(I) was synthesized as described by *Jothibasu* et al.[29] Chloro-(*N*,*N*-dimethylbenzimidazol-2-ylidene)gold(I) was synthesized as described by *Rodríguez-Castillo* et al.[30] Au(Dipp)Cl and Au(Mes)Cl were synthesized as described by Collado et al.[31] The synthesis for compounds **1**–**6** was adapted from *Garg* et al.[19] The synthesis for compounds **7**–**12** was adapted from Gao et al.[32] ^{1}H and ^{13}C NMR spectra were recorded on a Bruker AV400HD or a Bruker AV 500cryo spectrometer. ^{1}H and ^{13}C NMR spectra were referenced to the residual solvent signals.[33] Elemental analyses were done by the Microanalytical Laboratory at the Technical University of Munich.

The general procedure for the synthesis of benzimidazolyl-Au^{I}-alkynyl complexes **1**–**6** is shown in Scheme 3.

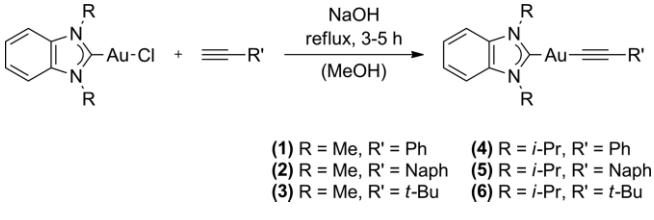

Scheme 3. General procedure for the synthesis of complexes **1**–**6**.

The corresponding alkyne and NaOH were dissolved in MeOH and heated to reflux for 15 minutes. The corresponding NHC-Au^{I}-Cl complex was added and heated to reflux for the time indicated. The suspension was evaporated to dryness, dissolved in DCM and extracted three times with water. The combined organic phases were dried with Na_2SO_4, filtered and the solvents evaporated to dryness. Compounds **3** and **5** needed additional purification steps, which are indicated at the corresponding entries.

(Me)BzImi-Au^{I}-(phenylethynyl) (1): A mixture of 17.4 µL phenylacetylene (16.9 mg, 158 µmol, 1 equiv.), 44.4 mg of NaOH (1.11 mmol, 7 equiv.) and 50.0 mg of chloro-(*N*,*N*-dimethylbenzimidazol-2-ylidene)gold(I) (132 µmol, 1 equiv.) was dissolved in 20 mL of MeOH and refluxed for three hours. Compound **1** was obtained as a white solid (52.8 mg, 119 µmol, 90 %). ^{1}H NMR (400 MHz, [D$_6$]DMSO): δ (ppm) = 7.76 (dd, $^{3}J_{H\text{-}H}$ = 6.1 Hz, ^{4}J = 3.2 Hz, 2H; $H_{ar(BzImi)}$), 7.49 (dd, $^{3}J_{H\text{-}H}$ = 6.1 Hz, 3.1 Hz, 2H; $H_{ar(BzImi)}$), 7.32–7.24 (m, 4H; $H_{ar(Ph)}$), 7.24–7.17 (m, 1H; $H_{ar(Ph)}$), 4.03 (s, 6H, H_{Me}); ^{13}C NMR (101 MHz, [D$_6$]DMSO): δ (ppm) = 193.0, 133.6, 133.4, 131.2, 128.2, 126.2, 126.1, 124.2, 111.8, 104.2, 34.6; elemental analysis calcd. (%) for $C_{17}H_{15}N_2Au$: C 45.96, H 3.40 N 6.31; found C 46.04 H 3.43 N 6.03.

(Me)BzImi-Au^{I}-(naphthylethynyl) (2): A mixture of 26.3 µL naphthylacetylene (28.1 mg, 185 µmol, 1 equiv.), 51.8 mg of NaOH (1.29 mmol, 7 equiv.) and 70.0 mg of chloro-(*N*,*N*-dimethylbenzimidazol-2-ylidene)gold(I) (185 µmol, 1 equiv.) was dissolved in 15 mL of MeOH and refluxed for four hours. Compound **2** was obtained as a slightly yellow solid (91.4 mg, 159 µmol, 86 %). Single crystals suitable for X-ray diffraction were obtained by slow diffusion of pentane into a solution of compound **2** in acetone. ^{1}H NMR (400 MHz, [D$_6$]DMSO): δ (ppm) = 8.45 (d, $^{3}J_{H\text{-}H}$ = 8.2 Hz, 1H; H_{naph}), 7.91 (d, $^{3}J_{H\text{-}H}$ = 7.2 Hz, 1H, H_{naph}), 7.81–7.74 (m, 3H, H_{naph}/$H_{ar(BzImi)}$), 7.61–7.47 (m, 5H, H_{naph}/$H_{ar(BzImi)}$), 7.43 (dd, $^{3}J_{H\text{-}H}$ = 8.2 Hz, 7.2 Hz 1H, H_{naph}), 4.07 (s, 6H, H_{Me}); ^{13}C NMR (101 MHz, [D$_6$]DMSO): δ (ppm) = 190.5, 133.4, 133.3, 132.9, 132.1, 129.2, 128.2, 126.5, 126.3, 126.2, 125.7, 124.0, 123.9, 113.3, 102.0, 52.9, 21.9; elemental analysis calcd. (%) for $C_{21}H_{17}N_2Au$: C 51.02, H 3.47 N 5.67; found C 50.83 H 3.47 N 5.42.

(Me)BzImi-Au^{I}-(*tert*-butylethynyl) (3): A mixture of 130 µL *tert*-butylacetylene (86.8 mg, 1.06 mmol, 5 equiv.), 59.2 mg of NaOH (1.48 mmol, 7 equiv.) and 80.0 mg of chloro-(*N*,*N*-dimethylbenzimidazol-2-ylidene)gold(I) (211 µmol, 1 equiv.) was dissolved in 15 mL of MeOH and refluxed for four hours. As a last purification step, the compound was dissolved in DCM and filtered through basic aluminium oxide. The filtrate was evaporated to dryness and compound **3** was obtained as a white solid (89.7 mg, 123 µmol, 58 %). ^{1}H NMR (400 MHz, [D$_6$]DMSO): δ (ppm) = 7.73 (dd, $^{3}J_{H\text{-}H}$ = 6.1 Hz, $^{4}J_{H\text{-}H}$ = 3.1 Hz, 2H, $H_{ar(BzImi)}$), 7.47 (dd, $^{3}J_{H\text{-}H}$ = 6.1 Hz, $^{3}J_{H\text{-}H}$ = 3.1 Hz, 2H, $H_{ar(BzImi)}$), 3.98 (s, 6H, $H_{Me(BzImi)}$), 1.15 (s, 9H, $H_{Me(alkynyl)}$). ^{13}C NMR (101 MHz, [D$_6$]DMSO): δ (ppm) = 194.0, 133.5, 124.1, 117.4, 112.9, 111.7, 99.5, 34.5, 32.2, 27.6; elemental analysis calcd. (%) for $C_{15}H_{19}N_2Au$: C 42.46, H 4.51 N 6.60; found C 42.15 H 4.47 N 6.58.

(*i*Pr)BzImi-Au^{I}-(phenylethynyl) (4): A mixture of 25.3 µL phenylacetylene (23.5 mg, 230 µmol, 1 equiv.), 64.4 mg of NaOH (1.61 mmol, 7 equiv.) and 100.0 mg of chloro(1,3-diisopropylbenzimidazolin-2-ylidene)gold(I) (230 µmol, 1 equiv.) was dissolved in 20 mL of MeOH and refluxed for three hours. Compound **4** was obtained as a white solid (63.1 mg, 127 µmol, 90 %). ^{1}H NMR (400 MHz, [D$_6$]DMSO): δ (ppm) = 7.96 (dd, $^{3}J_{H\text{-}H}$ = 6.2 Hz, $^{4}J_{H\text{-}H}$ = 3.2 Hz, 2H, $H_{ar(BzImi)}$), 7.43 (dd, $^{3}J_{H\text{-}H}$ = 6.2 Hz, $^{4}J_{H\text{-}H}$ = 3.2 Hz, 2H, $H_{ar(BzImi)}$), 7.34–7.24 (m, 4H, H_{Ph}), 7.22–7.16 (m, 1H, H_{Ph}), 5.38 (hept, $^{3}J_{H\text{-}H}$ = 7.0 Hz, 2H, H_{CH}), 1.72 (d, $^{3}J_{H\text{-}H}$ = 7.0, 12H, H_{Me}). ^{13}C NMR (101 MHz, [D$_6$]DMSO): δ (ppm) = 190.5, 132.6, 131.6, 131.2, 128.2, 126.2, 126.1, 124.0, 113.4, 104.5, 52.7, 21.9. elemental analysis calcd. (%) for $C_{21}H_{23}N_2Au$: C 50.41, H 4.63 N 5.60; found C 50.53 H 4.72 N 5.54.

(*i*Pr)BzImi-Au^{I}-(naphthylethynyl) (5): A mixture of 22.9 µL naphthylacetylene (24.5 mg, 161 µmol, 1 equiv.), 45.1 mg of NaOH (1.13 mmol, 7 equiv.) and 70.0 mg of chloro(1,3-diisopropylbenzimidazolin-2-ylidene)gold(I) (161 µmol, 1 equiv.) was dissolved in 15 mL of MeOH and refluxed for five hours. As a last purification step, the compound was dissolved in DCM and fractionally precipitated with pentane. The precipitate was washed with pentane (3×3 mL) and the solvents evaporated to dryness. Compound **5** was obtained as an off-white solid (49.8 mg, 90.2 µmol, 56 %). Single crystals suitable for X-ray diffraction were obtained by layering pentane on top of a solution of compound **5** in DCM. ^{1}H NMR (400 MHz, $CDCl_3$): δ (ppm) = 8.69 (d, $^{3}J_{H\text{-}H}$ = 7.5 Hz, 1H, H_{Naph}), 7.80 (d, $^{3}J_{H\text{-}H}$ = 8.1 Hz, 1H, H_{Naph}), 7.75 (dd, $^{3}J_{H\text{-}H}$ = 7.0 Hz, $^{4}J_{H\text{-}H}$ = 1.3 Hz, 1H, H_{Naph}), 7.70 (dd, $^{3}J_{H\text{-}H}$ = 7.0 Hz, $^{4}J_{H\text{-}H}$ = 1.3 Hz, 1H, H_{Naph}), 7.66 (dd, $^{3}J_{H\text{-}H}$ = 6.2, $^{4}J_{H\text{-}H}$ = 3.2 Hz, 2H, $H_{ar(BzImi)}$), 7.54 (ddd, $^{3}J_{H\text{-}H}$ = 8.1, 6.9 Hz, $^{4}J_{H\text{-}H}$ = 1.3 Hz, 1H, H_{Naph}), 7.47 (ddd, $^{4}J_{H\text{-}H}$ = 8.1, 6.9 Hz, $^{4}J_{H\text{-}H}$ = 1.3 Hz, 1H, H_{Naph}), 7.39 (d, $^{3}J_{H\text{-}H}$ = 7.5 Hz, 1H, H_{Naph}), 7.36 (dd, $^{3}J_{H\text{-}H}$ = 6.2 Hz, $^{4}J_{H\text{-}H}$ = 3.2 Hz, 2H, $H_{ar(BzImi)}$), 5.64 (hept, $^{3}J_{H\text{-}H}$ = 7.0 Hz, 2H, H_{CH}), 1.76 (d, $^{3}J_{H\text{-}H}$ = 7.0 Hz, 12H, H_{Me}). ^{13}C NMR (101 MHz, $CDCl_3$): δ (ppm) = 192.0, 134.0, 133.2, 133.0, 132.6, 130.4, 127.8, 127.4, 126.6, 125.8, 125.7, 125.2, 123.4, 113.1, 103.1, 53.9, 21.7; elemental analysis calcd. (%) for $C_{25}H_{25}N_2Au$: C 54.55, H 4.58 N 5.09; found C 54.14 H 4.63 N 5.07.

(*i*Pr)BzImi-Au^{I}-(*tert*-butylethynyl) (6): A mixture of 99.2 µL *tert*-butylacetylene (66.1 mg, 805 µmol, 5 equiv.), 45.1 mg of NaOH (1.13 mmol, 7 equiv.) and 70.0 mg of chloro(1,3-diisopropylbenzimidazolin-2-ylidene)gold(I) (161 µmol, 1 equiv.) was dissolved in 15 mL of MeOH and refluxed for four hours. Compound **6** was obtained as a white solid (54.3 mg, 113 µmol, 70 %). Single crystals suitable for X-ray diffraction were obtained by slow diffusion of pentane into a solution of compound **6** in acetone. ^{1}H NMR (400 MHz, [D_6]DMSO): δ (ppm) = 7.93 (dd, $^{3}J_{H\text{-}H}$ = 6.2 Hz, $^{4}J_{H\text{-}H}$ = 3.2 Hz, 2H, $H_{ar(BzImi)}$), 7.40 (dd, $^{3}J_{H\text{-}H}$ = 6.2 Hz, $^{4}J_{H\text{-}H}$ = 3.2 Hz, 2H, $H_{ar(BzImi)}$), 5.35 (hept, $^{3}J_{H\text{-}H}$ = 7.0 Hz, 2H, H_{CH}), 1.67 (d, $^{3}J_{H\text{-}H}$ = 7.0 Hz, 12H, $H_{Me(BzImi)}$), 1.15 (s, 9H, $H_{Me(alkynyl)}$). ^{13}C NMR (101 MHz, [D_6]DMSO): δ (ppm) = 191.6, 132.1, 123.9, 115.7, 113.3, 113.1, 55.0, 52.9, 32.3, 27.7, 21.7; elemental analysis calcd. (%) for $C_{19}H_{27}N_2Au$ C 47.50, H 5.67 N 5.83; found C 47.33 H 5.67 N 5.72.

The general procedure for the synthesis of 1,3-dihydroimidazolylidene-Au^{I}-alkynyl complexes **7**–**12** is shown in Scheme 4.

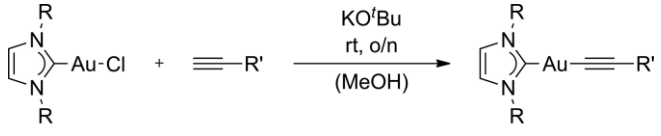

(7) R = Mes, R' = Ph **(10)** R = Dipp, R' = Ph
(8) R = Mes, R' = Naph **(11)** R = Dipp, R' = Naph
(9) R = Mes, R' = *t*-Bu **(12)** R = Dipp, R' = *t*-Bu

Scheme 4. General procedure for the synthesis of complexes **7**–**12**.

Potassium *tert*-butoxide was dissolved in MeOH and the corresponding alkyne was added and stirred at room temperature for 5 min. Meanwhile, a suspension of the corresponding NHC-Au^{I}-Cl compound in MeOH was prepared in a separate flask and stirred at room temperature. The solution containing potassium *tert*-butoxide and the alkyne was then added dropwise to the suspension containing the NHC-Au^{I}-Cl compound and stirred at room temperature overnight. The solution was evaporated to dryness, redissolved in either DCM or Et_2O, **filtered through** Celite an evaporated to dryness. Compounds **8** and **11** needed additional purification steps, which are indicated at the corresponding entries.

(Mes)-Au^{I}-(phenylethynyl) (7): 31.4 mg of potassium *tert*-butoxide (279 µmol, 3 equiv.) and 30.7 µL phenylacetylene (28.5 mg, 279 µmol, 3 equiv.) were dissolved in 2 mL of MeOH. In a separate flask, 50.0 mg of Au(IMes)Cl (93.1 µmol, 1 equiv.) were suspended in 2 mL of MeOH. After dropwise addition of the first solution to the second, the resulting solution was stirred at room temperature for overnight. The solution was evaporated to dryness, redissolved in Et_2O and filtered through Celite. Evaporating the solution to dryness yielded compound **7** as an off-white solid (24.2 mg, 40.1 µmol, 43 %). ^{1}H NMR (400 MHz, [D_6]DMSO): δ (ppm) = 7.76 (s, 2H, $H_{ar(Imi)}$), 7.21–7.06 (m, 9H, $H_{ar(Mes)}$/$H_{ar(Ph)}$), 2.35 (s, 6H, H_{Me}), 2.08 (s, 12H, H_{Me}). ^{13}C NMR (101 MHz, [D_6]DMSO): δ (ppm) = 87.2, 139.4, 135.5, 135.0, 133.4, 132.3, 131.4, 129.5, 128.6, 126.4, 123.9, 103.8, 21.2, 17.7; elemental analysis calcd. (%) for $C_{29}H_{29}N_2Au$ C 57.81, H 4.85 N 4.65; found C 57.78 H 4.86 N 4.50.

(Mes)-Au^{I}-(naphthylethynyl) (8): 31.4 mg of potassium *tert*-butoxide (279 µmol, 3 equiv.) and 39.7 µL naphthylacetylene (42.5 mg, 279 µmol, 3 equiv.) were dissolved in 2 mL of MeOH. In a separate flask, 50.0 mg of Au(IMes)Cl (93.1 µmol, 1 equiv.) were suspended in 2 mL of MeOH. After dropwise addition of the first solution to the second, the resulting solution was stirred at room temperature for overnight. The solution was evaporated to dryness, redissolved in DCM and filtered through Celite. Fractional precipitation with pentane yielded compound **8** as an off-white solid (19.6 mg, 29.8 µmol, 32 %). Single crystals suitable for X-ray diffraction were obtained by slow diffusion of pentane into a solution of compound **8** in benzene. ^{1}H NMR (400 MHz, [D_6]DMSO): δ (ppm) = 8.19–8.11 (m, 1H, H_{Naph}), 7.86–7.81 (m, 1H, H_{Naph}), 7.77 (s, 2H, $H_{ar(Imi)}$), 7.70–7.66 (m, 1H, H_{Naph}), 7.50–7.45 (m, 2H, H_{Naph}), 7.37–7.28 (m, 2H, $H_{ar(Mes)}$), 7.14 (s, 4H, $H_{ar(Mes)}$), 2.34 (s, 6H, H_{Me}), 2.11 (s, 12H, H_{Me}). ^{13}C NMR (101 MHz, [D_6]DMSO): δ (ppm) = 186.6, 139.0, 138.5, 135.1, 134.6, 133.1, 132.8, 129.1, 128.1, 126.3, 126.1, 125.6, 123.7, 123.6, 100.9, 30.8, 20.8, 17.4; elemental analysis calcd. (%) for $C_{33}H_{31}N_2Au$: C 60.74, H 4.79 N 4.29; found C 60.60 H 4.95 N 4.02.

(Mes)-Au^{I}-(*tert*-butylethynyl) (9): 31.4 mg of potassium *tert*-butoxide (279 µmol, 3 equiv.) and 34.4 µL *tert*-butylacetylene (23.0 mg, 279 µmol, 3 equiv.) were dissolved in 2 mL of MeOH. In a separate flask, 50.0 mg of Au(IMes)Cl (93.1 µmol, 1 equiv.) were suspended in 2 mL of MeOH. After dropwise addition of the first solution to the second, the resulting solution was stirred at room temperature for overnight. The solution was evaporated to dryness, redissolved in Et_2O and filtered through Celite. Evaporating the solution to dryness yielded compound **9** as a white solid (45.6 mg, 78.2 µmol, 84 %). Single crystals suitable for X-ray diffraction were obtained by slow diffusion of pentane into a solution of compound **9** in benzene. ^{1}H NMR (400 MHz, [D_6]DMSO): δ (ppm) = (s, 2H, $H_{ar(Imi)}$), 7.10 (m, 4H, $H_{ar(Mes)}$), 2.33 (s, 6H, $H_{Me(Mes)}$), 2.04 (s, 12H, $H_{Me(Mes)}$), 0.97 (s, 9H, $H_{Me(alkynyl)}$). ^{13}C NMR (101 MHz, [D_6]DMSO, 298 K): δ (ppm) = 186.6, 139.0, 138.5, 135.1, 134.6, 133.1, 132.8, 129.1, 128.1, 126.3, 126.1, 125.6, 123.7, 123.6, 100.9, 30.8, 20.8, 17.4; elemental analysis calcd. (%) for $C_{27}H_{33}N_2Au$: C 55.67, H 5.71 N 4.81 Found: C 55.32 H 5.72 N 4.79.

(Dipp)-Au^{I}-(phenylethynyl) (10): 27.1 mg of potassium *tert*-butoxide (242 µmol, 3 equiv.) and 26.5 µL phenylacetylene (24.7 mg, 242 µmol, 3 equiv.) were dissolved in 2 mL of MeOH. In a separate flask, 50.0 mg of Au(dipp)Cl (80.5 µmol, 1 equiv.) were suspended in 2 mL of MeOH. After dropwise addition of the first solution to the second, the resulting solution was stirred at room temperature for overnight. The solution was evaporated to dryness, redissolved in Et_2O and filtered through Celite. Evaporating the solution to dryness and trituration with pentane yielded compound **10** as a white solid (29.0 mg, 41.9 µmol, 52 %). ^{1}H NMR (500 MHz, [D_6]DMSO,

298 K): δ (ppm) = 7.90 (s, 2H, $H_{ar(Imi)}$), 7.56 (t, ^3J = 7.8 Hz 2H, $H_{ar(dipp)}$), 7.41 (d, $^3J_{H-H}$ = 7.8 Hz, 4H, $H_{ar(dipp)}$), 7.16–7.03 (m, 5H, H_{Ph}), 2.54–2.52 (m, 4H, $H_{CH(iPr)}$), 1.27 (d, $^3J_{H-H}$ = 6.8 Hz, 12H, $H_{Me(iPr)}$), 1.20 (d, $^3J_{H-H}$ = 6.8 Hz, 12H, $H_{Me(iPr)}$). ^{13}C NMR (101 MHz, [D_6]DMSO): δ (ppm) = 188.5, 145.4, 134.3, 132.4, 131.1, 130.4, 128.0, 126.0, 125.9, 124.6, 124.0, 103.3, 28.4, 24.3, 23.5; elemental analysis calcd. (%) for $C_{35}H_{41}N_2Au$: C 61.22, H 6.02 N 4.08 Found: C 60.99 H 5.98 N 4.00.

(Dipp)-Au^I-(naphthylethynyl) (11): 27.1 mg of potassium *tert*-butoxide (242 µmol, 3 equiv.) and 34.4 µL naphylacetylene (36.8 mg, 242 µmol, 3 equiv.) were dissolved in 2 mL of MeOH. In a separate flask, 50.0 mg of Au(dipp)Cl (80.5 µmol, 1 equiv.) were suspended in 2 mL of MeOH. After dropwise addition of the first solution to the second, the resulting solution was stirred at room temperature for overnight. The solution was evaporated to dryness, redissolved in DCM and filtered through Celite. Fractional precipitation with pentane yielded compound **11** as a white solid (16.3 mg, 21.8 µmol, 27 %). ^{1}H NMR (400 MHz, [D_6]DMSO): δ (ppm) = 8.12–8.07 (m, 1H, H_{Naph}), 7.96 (s, 2H, $H_{ar(Imi)}$), 7.84–7.80 (m, 1H, H_{Naph}), 7.69–7.64 (m, 1H, H_{Naph}), 7.60–7.55 (m, 2H, $H_{ar(dipp)}$), 7.46–7.41 (m, 6H, $H_{ar(dipp)}$), 7.31–7.28 (m, 2H, H_{Naph}), 2.56 (hept, $^3J_{H-H}$ = 6.8 Hz, 4H, $H_{CH(iPr)}$), 1.34 (d, $^3J_{H-H}$ = 6.8 Hz, 12H, $H_{Me(iPr)}$), 1.23 (d, $^3J_{H-H}$ = 6.8 Hz, 12H, $H_{Me(iPr)}$). ^{13}C NMR (101 MHz, [D_6]DMSO): δ (ppm) = 188.5, 145.4, 138.3, 134.3, 133.2, 132.8, 130.4, 128.8, 128.1, 126.2, 126.0, 125.5, 124.7, 124.0, 123.7, 109.6, 101.0, 28.4, 24.3, 23.6; elemental analysis calcd. (%) for $C_{39}H_{43}N_2Au$: C 63.58, H 5.88 N 3.80; found C 63.63 H 5.90 N 3.77.

(Dipp)-Au^I-(*tert*-butylethynyl) (12): 27.1 mg of potassium *tert*-butoxide (242 µmol, 3 equiv.) and 29.8 µL *tert*-butylacetylene (19.8 mg, 242 µmol, 3 equiv.) were dissolved in 2 mL of MeOH. In a separate flask, 50.0 mg of Au(dipp)Cl (80.5 µmol, 1 equiv.) were suspended in 2 mL of MeOH. After dropwise addition of the first solution to the second, the resulting solution was stirred at room temperature for overnight. The solution was evaporated to dryness, redissolved in Et_2O and filtered through Celite. Evaporating the solution to dryness yielded compound **12** as a white solid (42.4 mg, 63.6 µmol, 79 %). ^{1}H NMR (400 MHz, [D_6]DMSO): δ (ppm) = 7.87 (s, 2H, $H_{ar(Imi)}$), 7.55 (t, $^3J_{H-H}$ = 7.8 Hz, 2H, $H_{ar(dipp)}$), 7.41 (d, $^3J_{H-H}$ = 7.8 Hz, 4H, $H_{ar(dipp)}$), 2.54–2.52 (m, 4H, $H_{CH(iPr)}$), 1.26 (d, $^3J_{H-H}$ = 6.9 Hz, 12H, $H_{Me(iPr)}$), 1.19 (d, $^3J_{H-H}$ = 6.9 Hz, 12H, $H_{Me(iPr)}$), 0.96 (s, 9H, $H_{Me(alkynyl)}$). ^{13}C NMR (101 MHz, [D_6]DMSO): δ (ppm) = 189.4, 145.3, 134.5, 130.3, 124.5, 124.0, 116.0, 111.4, 32.2, 28.4, 27.4, 24.3, 23.5; elemental analysis calcd. (%) for $C_{33}H_{45}N_2Au$: C 59.45, H 6.80 N 4.20; found C 59.37 H 6.89 N 4.25.

Single Crystal X-ray Diffraction

Data were collected on a single-crystal X-ray diffractometer equipped with a CMOS detector (Photon 100), a rotating anode TXS and a Helios mirror optic using the APEX3 software package (**2**, **6**, **8** and **9**) or a single-crystal X-ray diffractometer equipped with a CMOS detector (Bruker APEX III, κ-CMOS), an IMS microsource with Mo-K_α radiation (λ = 0.71073 Å) and a Helios optic using the APEX3 software package(**5**).[34] Measurements were performed on single crystals coated with perfluorinated ether. The crystals were fixed on top of a kapton micro sampler and frozen under a stream of cold nitrogen. A matrix scan was used to determine the initial lattice parameters. Reflections were corrected for Lorentz and polarisation effects, scan speed, and background using SAINT.[35] Absorption correction, including odd and even ordered spherical harmonics was performed using SADABS or TWINABS.[36] Space group assignment was based upon systematic absences, E statistics, and successful refinement of the structure. The structures were solved using SHELXS or SHELXT with the aid of successive difference Fourier maps, and were refined against all data using SHELXL in conjunction with SHELXLE.[37,38] Hydrogen atoms were calculated in ideal positions as follows: Methyl hydrogen atoms were refined as part of rigid rotating groups, with a C–H distance of 0.98 Å and $U_{iso(H)}$ = 1.5•$U_{eq(C)}$. Other H atoms were placed in calculated positions and refined using a riding model, with methylene and aromatic C–H distances of 0.99 Å and 0.95 Å, respectively, and other C–H distances of 1.00 Å, all with $U_{iso(H)}$ = 1.2•$U_{eq(C)}$. Non-hydrogen atoms were refined with anisotropic displacement parameters. Full-matrix least-squares refinements were carried out by minimizing $\Sigma w(F_o^2 - F_c^2)^2$ with the SHELXL weighting scheme[38] Neutral atom scattering factors for all atoms and anomalous dispersion corrections for the non-hydrogen atoms were taken from *International Tables for Crystallography*.[39] A split layer refinement was used for disordered groups and additional restraints (SHELXL: SIMU, DELU and RIGU) were used, if necessary. Images of the crystal structures were generated with PLATON.[40]

CCDC 1955875 (for **2**), 1955877 (for **5**), 1955879 (for **6**), 1955876 (for **8**), and 1955878 (for **9**) contain the supplementary crystallographic data for this paper. These data can be obtained free of charge from The Cambridge Crystallographic Data Centre.

Stability and Reactivity Studies: The stability of compounds **1**–**12** in H_2O was evaluated by dissolving 6 µmol of the respective compound in 0.5 mL of [D_6]DMSO/D_2O (80:20). The reactivity against EtSH was investigated by dissolving 6 µmol of compounds **1**–**12** in 0.5 mL of [D_6]DMSO and addition of an excess of EtSH and D_2O (approximately 300 µmol each). Dry EtSH was obtained by fractional distillation of EtSH and drying over molecular sieves (3 Å). Stability and reactivity were checked by ^{1}H NMR spectroscopy over several days.

Quantum Mechanical Calculations: Density functional theory (DFT) computations were carried out using the Gaussian 09 package. The structures were optimized on the B3LYP level of theory[41] and employing the def2-SVP basis set.[42] Subsequently, single point energy calculations were performed on the B3LYP/def2-TZVP[42,43] and the M062X/def2-TZVP[44] level to ensure comparability of functionals and basis sets. For M062X/def2-TZVP additional single point energy calculations have been performed in the presence of dimethyl sulfoxide using a self-consistent reaction field (SCRF).[45] DFT exploration of potential energy surfaces started from plausible geometries for separate reactants that were fully geometry optimized without any constraints and confirmed as minima by harmonic frequency calculation. Relaxed potential energy scans were then performed for several reaction coordinates [Au–S, Au–C(alkynyl), Au–C(NHC), C(alkynyl)–H(H_2O)], from which approximate geometries of transition states were extracted manually. Several possible reaction coordinates were tested for each reaction step, from which several possible transition state geometries were tested. Accurate transition state geometries were then obtained by optimization of the approximate geometries. All optimized geometries were checked by frequency determination for negative eigenfrequencies, corresponding to the local minima (stable compounds) or the local maxima (transition states) on the potential energy hypersurfaces. Transition states were additionally checked by intrinsic reaction coordinate (IRC) calculations.[46] Those reported in the paper are the ones with lowest energy that properly connect the required reactants and products.

UV-Visible Absorption Spectroscopy: UV-Visible absorption spectra to investigate the stability of compounds **1**–**12** in solution were recorded on a Cary 60 UV-Vis spectrometer (Agilent Technologies, Santa Clara, USA). A stock solution of compounds was prepared in DMSO. An aliquot was diluted to ca. 20 µM in 1 × PBS (pH 7.4), and the UV-Visible spectra acquired at room temperature over 24 h at

different intervals (every 15 min during the first hour and every hour for the remaining 23 h).

FRET DNA Melting Assay: Fluorescence resonance energy transfer (FRET) experiments were run on an Applied Biosystems® Quantum-Studio 5 Real-Time PCR thermocycler (Thermo Fisher Scientific, Waltham, USA) equipped with a FAM filter (λ_{ex} = 492 nm; λ_{em} = 516 nm). The thermocycler was set to perform a stepwise increase of 0.3 °C every 30 s, from 25 °C to 95 °C, and measurements were acquired after each step.

All the oligonucleotides were purchased from Eurogentec (Belgium) in HPLC purity grade. The FRET probes used were FAM (6-carboxy-fluorescein) and TAMRA (6-carboxy-tetramethylrhodamine). The lyophilized fluorolabelled hTelo (21-mer), d[GGG(TTAGGG)3], *C-KIT1*, d[GGGAGGGCGCTGGGAGGAGGG] oligonucleotides were firstly diluted in deionized water to obtain 100 μM stock solutions. Stock solutions were diluted to a concentration of 400 nM in potassium cacodylate buffer (60 mM, pH 7.4), and then annealed to form G-quadruplex (G4) structures by heating to 95 °C for 5 min, followed by cooling to room temperature overnight. Experiments were carried out in a 96-well plate with a total volume of 30 μL. The final concentration of the G4-oligonucleotide was set to 200 nM in potassium cacodylate buffer (60 mM, pH 7.4). Stock solutions of the gold compounds in DMSO (1 mM) were freshly prepared prior to the experiments. The stock solutions were further diluted to a final concentration of 2 μM (with a total percentage of DMSO of approx. 0.1 %) in potassium cacodylate buffer (60 mM, pH 7.4) to achieve G4/gold compound stoichiometry of 1:5.

Cell Lines and Culture Maintenance: The human cancer cell lines corresponding to breast carcinoma (MCF-7), ovarian adenocarcinoma (SKOV-3) and skin malignant melanoma (A375) were obtained from the ATCC. The SKOV-3 and A375 cells were cultured in Dulbecco's Modified Eagle Medium (DMEM, 4.5 g/L glucose, Corning), supplemented with 10 % fetal bovine serum (One-Shot FBS, EU-approved South American Origin, Thermo Fisher Scientific) and 1 % penicillin/streptomycin (Gibco). MCF-7 cells were grown in Roswell Park Memorial Institute medium (RPMI, L-glutamine, Corning), supplemented with 10 % fetal bovine serum (One Shot FBS, EU-approved South American Origin, Thermo Fisher Scientific) and 1 % penicillin/streptomycin (Gibco). All cell lines were cultured at 37 °C, in a humidified atmosphere of 5 % CO_2 and passage diluted upon reaching confluence.

Antiproliferative Assays: To evaluate the inhibition of cell growth by the gold complexes, cells were seeded in 96-well tissue culture-treated plates (Corning) at 8'000 cells/well in 200 μL complete medium. Working solutions of the gold compounds were prepared in the required concentration by diluting freshly prepared stock solutions (10^{-2} M in DMSO) in complete medium. The stock solutions were protected from light in order to avoid potential light-induced degradation. Cells were allowed to adhere for 24 h. Then, the medium was refreshed and cells were incubated for 72 h in 200 μL complete medium containing different concentrations of the gold compounds. The antiproliferative effects of complexes were evaluated using the 3-(4,5-dimethylthiazol-2-yl)-2,5-diphenyltetrazolium bromide (MTT) assay. Following 72 h exposure, the medium was removed and 3-(4,5-dimethylthiazol-2-yl)-2,5-diphenyltetrazolium bromide (MTT, Fluorochem) in 10 × PBS (Corning) was added to the cells, at a final concentration of 0.3 mg/mL. After 3–4 h incubation at 37 °C and 5 % CO_2, the supernatant was discarded and the formazan crystals were dissolved with DMSO. The optical density was quantified in quadruplicates for each experiment at 550 nm using a multi-well plate reader (VICTOR X, Perking Elmer). The EC_{50} value for each compound in both assays was calculated as the concentration showing 50 % decrease in cell growth, when compared to controls, using a nonlinear fitting. Data is presented as mean ± standard deviation of at least three independent experiments.

Acknowledgments

A. C. acknowledges support from Cardiff University. Authors acknowledge the Hans Fischer Senior Fellowship of the Technical University of Munich-Institute for Advanced Study, funded by the German Excellence Initiative and the European Union Seventh Framework Programme under grant agreement No. 291763. R. B. acknowledges funding from the European Union's Horizon 2020 research and innovation programme under the Marie Skłodowska-Curie grant agreement No. 663830.

Keywords: Gold · N-heterocyclic carbenes · Alkyne ligands · Thiols · G-quadruplexes · Antitumor agents

[1] B. W. Stewart, C. Wild (Eds.) *World cancer report* ***2014***, International Agency for Research on Cancer, Lyon, France, **2014**.
[2] L. Kelland, *Nat. Rev. Cancer* **2007**, *7*, 573–584.
[3] A. Casini, Medicinal chemistry of gold anticancer metallodrugs. In: (Eds.: A. Sigel, et al.), Metallo-Drugs: Development and Action of Anticancer Agents, Vol. 18. Metal Ions in Life Sciences Walter de Gruyter GmbH, pp. 199–217. (Ed.), **2018**.
[4] B. Bertrand, A. Casini, *Dalton Trans.* **2014**, *43*, 4209–4219.
[5] a) A. Casini, Medicinal chemistry of gold anticancer metallodrugs. In: (Eds.: A. Sigel, et al.), Metallo-Drugs: Development and Action of Anticancer Agents. **2018**, Vol. 18. Metal Ions in Life Sciences Walter de Gruyter GmbH, pp. 199–217; b) A. Casini, R. Bonsignore, J. Oberkofler, *Organometallic gold-based anticancer therapeutics* (Ed.) Reference Module in Chemistry, Molecular Sciences and Chemical Engineering, Elsevier, pp. 1–12, **2018**; c) M. Porchia, M. Pellei, M. Marinelli, F. Tisato, F. Del Bello, C. Santini, *Eur. J. Med. Chem.* **2018**, *146*, 709–746.
[6] M. Mora, M. C. Gimeno, R. Visbal, *Chem. Soc. Rev.* **2019**, *48*, 447–462.
[7] T. Zou, C.-N. Lok, P.-K. Wan, Z.-F. Zhang, S.-K. Fung, C.-M. Che, *Curr. Opin. Chem. Biol.* **2018**, *43*, 30–36.
[8] a) C. Zhang, M.-L. Maddelein, R. Wai-Yin Sun, H. Gornitzka, O. Cuvillier, C. Hemmert, *Eur. J. Med. Chem.* **2018**, *157*, 320–332; b) C. Zhang, C. Hemmert, H. Gornitzka, O. Cuvillier, M. Zhang, R. W.-Y. Sun, *ChemMedChem* **2018**, *13*, 1218–1229; c) Ö. Karaca, V. Scalcon, S. M. Meier-Menches, R. Bonsignore, J. M. J. L. Brouwer, F. Tonolo, A. Folda, M. P. Rigobello, F. E. Kühn, A. Casini, *Inorg. Chem.* **2017**, *56*, 14237–14250; d) W. Niu, X. Chen, W. Tan, A. S. Veige, *Angew. Chem. Int. Ed.* **2016**, *55*, 8889–8893; *Angew. Chem.* **2016**, *128*, 9035; e) B. Bertrand, E. Bodio, P. Richard, M. Picquet, P. Le Gendre, A. Casini, *J. Organomet. Chem.* **2015**, *775*, 124–129.
[9] W. Liu, R. Gust, *Coord. Chem. Rev.* **2016**, *329*, 191–213.
[10] a) A. Bindoli, M. P. Rigobello, G. Scutari, C. Gabbiani, A. Casini, L. Messori, *Coord. Chem. Rev.* **2009**, *253*, 1692–1707; b) C. Schmidt, B. Karge, R. Misgeld, A. Prokop, R. Franke, M. Brönstrup, I. Ott, *Chem. Eur. J.* **2017**, *23*, 1869–1880; c) E. Schuh, C. Pflüger, A. Citta, A. Folda, M. P. Rigobello, A. Bindoli, A. Casini, F. Mohr, *J. Med. Chem.* **2012**, *55*, 5518–5528; d) R. Rubbiani, S. Can, I. Kitanovic, H. Alborzinia, M. Stefanopoulou, M. Kokoschka, S. Mönchgesang, W. S. Sheldrick, S. Wölfl, I. Ott, *J. Med. Chem.* **2011**, *54*, 8646–8657.
[11] a) F. Mendes, M. Groessl, A. A. Nazarov, Y. O. Tsybin, G. Sava, I. Santos, P. J. Dyson, A. Casini, *J. Med. Chem.* **2011**, *54*, 2196–2206; b) Ü. A. Laskay, C. Garino, Y. O. Tsybin, L. Salassa, A. Casini, *Chem. Commun.* **2015**, *51*, 1612–1615; c) M. N. Wenzel, R. Bonsignore, S. R. Thomas, D. Bourissou, G. Barone, A. Casini, *Chem. Eur. J.* **2019**, *25*, 7628–7634; d) C. Abbehausen, R. E. F. de Paiva, R. Bjornsson, S. Q. Gomes, Z. Du, P. P. Corbi, F. A. Lima, N. Farrell, *Inorg. Chem.* **2018**, *57*, 218–230.
[12] a) B. Aikman, A. de Almeida, S. M. Meier-Menches, A. Casini, *Metallomics* **2018**, *10*, 696–712; b) M. N. Wenzel, A. F. Mósca, V. Graziani, B. Aikman, S. R. Thomas, A. de Almeida, J. A. Platts, N. Re, C. Coletti, A. Marrone, et al., *Inorg. Chem.* **2019**, *58*, 2140–2148.

[13] A. de Almeida, B. L. Oliveira, J. D. G. Correia, G. Soveral, A. Casini, *Coord. Chem. Rev.* **2013**, *257*, 2689–2704.
[14] Ö. Karaca, S. M. Meier-Menches, A. Casini, F. E. Kühn, *Chem. Commun.* **2017**, *53*, 8249–8260.
[15] a) B. Bertrand, L. Stefan, M. Pirrotta, D. Monchaud, E. Bodio, P. Richard, P. Le Gendre, E. Warmerdam, M. H. de Jager, G. M. M. Groothuis, et al., *Inorg. Chem.* **2014**, *53*, 2296–2303; b) C. Bazzicalupi, M. Ferraroni, F. Papi, L. Massai, B. Bertrand, L. Messori, P. Gratteri, A. Casini, *Angew. Chem. Int. Ed.* **2016**, *55*, 4256–4259; *Angew. Chem.* **2016**, *128*, 4328.
[16] N. Estrada-Ortiz, F. Guarra, I. A. M. de Graaf, L. Marchetti, M. H. de Jager, G. M. M. Groothuis, C. Gabbiani, A. Casini, *ChemMedChem* **2017**, *12*, 1429–1435.
[17] S. M. Meier-Menches, B. Aikman, D. Döllerer, W. T. Klooster, S. J. Coles, N. Santi, L. Luk, A. Casini, R. Bonsignore, *J. Inorg. Biochem.* **2019**, 110844.
[18] H. M. J. Wang, C. Y. L. Chen, I. J. B. Lin, *Organometallics* **1999**, *18*, 1216–1223.
[19] J. A. Garg, O. Blacque, J. Heier, K. Venkatesan, *Eur. J. Inorg. Chem.* **2012**, *2012*, 1750–1763.
[20] L. Canovese, C. Levi, F. Visentin, C. Santo, V. Bertolasi, *Inorg. Chim. Acta* **2013**, *404*, 105–112.
[21] S. Gaillard, A. M. Z. Slawin, S. P. Nolan, *Chem. Commun.* **2010**, *46*, 2742–2744.
[22] J. E. Heckler, N. Deligonul, A. L. Rheingold, T. G. Gray, *Chem. Commun.* **2013**, *49*, 5990–5992.
[23] a) R. Dorel, A. M. Echavarren, *Chem. Rev.* **2015**, *115*, 9028–9072; b) J. Bucher, T. Wurm, K. S. Nalivela, M. Rudolph, F. Rominger, A. S. K. Hashmi, *Angew. Chem. Int. Ed.* **2014**, *53*, 3854–3858; *Angew. Chem.* **2014**, *126*, 3934; c) Y. Wang, Z. Wang, Y. Li, G. Wu, Z. Cao, L. Zhang, *Nat. Commun.* **2014**, *5*, 3470.
[24] J. L. Hickey, R. A. Ruhayel, P. J. Barnard, M. V. Baker, S. J. Berners-Price, A. Filipovska, *J. Am. Chem. Soc.* **2008**, *130*, 12570–12571.
[25] a) K. Köhler, S. J. Silverio, I. Hyla-Kryspin, R. Gleiter, L. Zsolnai, A. Driess, G. Huttner, H. Lang, *Organometallics* **1997**, *16*, 4970–4979; b) P. Schulte, U. Behrens, *Chem. Commun.* **1998**, 1633–1634; c) H. V. R. Dias, J. A. Flores, J. Wu, P. Kroll, *J. Am. Chem. Soc.* **2009**, *131*, 11249–11255.
[26] I. Tolbatov, C. Coletti, A. Marrone, N. Re, *Int. J. Mol. Sci.* **2019**, *20*, 820.
[27] X. Zhou, L. Zhou, *Theor. Chem. Acc.* **2016**, *135*, 921.
[28] a) T. V. Serebryanskaya, A. A. Zolotarev, I. Ott, *Med. Chem. Commun.* **2015**, *6*, 1186–1189; b) W. F. Gabrielli, S. D. Nogai, M. Nell, S. Cronje, H. G. Raubenheimer, *Polyhedron* **2012**, *34*, 188–197.
[29] R. Jothibasu, H. V. Huynh, L. L. Koh, *J. Organomet. Chem.* **2008**, *693*, 374–380.
[30] M. Rodríguez-Castillo, D. Laurencin, F. Tielens, A. van der Lee, S. Clément, Y. Guari, S. Richeter, *Dalton Trans.* **2014**, *43*, 5978–5982.
[31] A. Collado, A. Gómez-Suárez, A. R. Martin, A. M. Z. Slawin, S. P. Nolan, *Chem. Commun.* **2013**, *49*, 5541–5543.
[32] L. Gao, D. V. Partyka, J. B. Updegraff, N. Deligonul, T. G. Gray, *Eur. J. Inorg. Chem.* **2009**, *2009*, 2711–2719.
[33] G. R. Fulmer, A. J. M. Miller, N. H. Sherden, H. E. Gottlieb, A. Nudelman, B. M. Stoltz, J. E. Bercaw, K. I. Goldberg, *Organometallics* **2010**, *29*, 2176–2179.
[34] *APEX suite of crystallographic software*, APEX 3, Version **2015**–5.2, Bruker AXS Inc., Madison, Wisconsin, USA, 2014/2015.
[35] *SAINT*, Versions 8.32B, 8.34A and 8.38A, Bruker AXS Inc., Madison, Wisconsin, USA, **2012**/2014/2017.
[36] a) *SADABS*, Versions **2012**/1, 2014/5 and 2016/2, Bruker AXS Inc., Madison, Wisconsin, USA, 2012/2014/2016; b) *TWINABS*, Versions **2012**/1, Bruker AXS Inc., Madison, Wisconsin, USA, 2012.
[37] a) G. M. Sheldrick, *Acta Crystallogr., Sect. C* **2015**, *71*, 3–8; b) C. B. Hübschle, G. M. Sheldrick, B. Dittrich, *J. Appl. Crystallogr.* **2011**, *44*, 1281–1284.
[38] G. M. Sheldrick, *Acta Crystallogr., Sect. A* **2015**, *71*, 3–8.
[39] *International Tables for Crystallography*, Vol. C (Ed.: A. J. Wilson), Kluwer Academic Publishers, Dordrecht, The Netherlands, **1992**, Tables 6.1.1.4 (pp. 500–502), 4.2.6.8 (pp. 219–222), and 4.2.4.2 (pp. 193–199).
[40] A. L. Spek, *Acta Crystallogr., Sect. D* **2009**, *65*, 148–155.
[41] a) A. D. Becke, *Phys. Rev. A* **1988**, *38*, 3098–3100; b) A. D. Becke, *J. Chem. Phys.* **1993**, *98*, 5648–5652; c) C. Lee, W. Yang, R. G. Parr, *Phys. Rev. B* **1988**, *37*, 785–789; d) P. J. Stephens, F. J. Devlin, C. F. Chabalowski, M. J. Frisch, *J. Phys. Chem.* **1994**, *98*, 11623–11627.
[42] F. Weigend, R. Ahlrichs, *Phys. Chem. Chem. Phys.* **2005**, *7*, 3297–3305.
[43] F. Weigend, *Phys. Chem. Chem. Phys.* **2006**, *8*, 1057–1065.
[44] Y. Zhao, D. G. Truhlar, *Theor. Chem. Acc.* **2008**, *120*, 215–241.
[45] J. Tomasi, B. Mennucci, R. Cammi, *Chem. Rev.* **2005**, *105*, 2999–3093.
[46] K. Fukui, *Acc. Chem. Res.* **1981**, *14*, 363–368.

Received: September 27, 2019